Shutoff and Agonist-Triggered Internalization of Protease-Activated Receptor 1 Can Be Separated by Mutation of Putative Phosphorylation Sites in the Cytoplasmic Tail†

Stephen R. Hammes,[‡,§,||] Michael J. Shapiro,[‡] and Shaun R. Coughlin*[,‡,||,⊥]

Cardiovascular Research Institute, Division of Endocrinology, Department of Medicine, and Department of Cellular and Molecular Pharmacology, University of California, San Francisco, 505 Parnassus Avenue, San Francisco, California 94143-0130

Received January 29, 1999; Revised Manuscript Received May 17, 1999

ABSTRACT: The thrombin receptor PAR1 becomes rapidly phosphorylated upon activation by either thrombin or exogenous SFLLRN agonist peptide. Substitution of alanine for all serine and threonine residues in the receptor's cytoplasmic carboxyl-terminal tail ablated phosphorylation and yielded a receptor defective in both shutoff and agonist-triggered internalization. These observations suggested that activation-dependent phosphorylation of PAR1's cytoplasmic tail is required for both shutoff and agonist-triggered internalization. To identify the phosphorylation site(s) that are necessary for these functions, we generated three mutant receptors in which alanine was substituted for serine and threonine residues in the amino-terminal, middle, and carboxyl-terminal thirds of PAR1's cytoplasmic tail. When stably expressed in fibroblasts, all three mutated receptors were rapidly phosphorylated in response to agonist, while a mutant in which all serines and threonines in the cytoplasmic tail were converted to alanines was not. This result suggests that phosphorylation can occur at multiple sites in PAR1's cytoplasmic tail. Alanine substitutions in the N-terminal and C-terminal portions of the tail had no effect on either receptor shutoff or agonist-triggered internalization. By contrast, alanine substitutions in the "middle" serine cluster between Ser^{391} and Ser^{406} yielded a receptor with considerably slower shutoff of signaling after thrombin activation than the wild type. Surprisingly, this same mutant was indistinguishable from the wild type in agonist-triggered internalization and degradation. Overexpression of G protein-coupled receptor kinase 2 (GRK2) and GRK3 "suppressed" the shutoff defect of the S → A (391−406) mutant, consistent with this defect being due to altered receptor phosphorylation. These results suggest that specific phosphorylation sites are required for rapid receptor shutoff, but phosphorylation at multiple alternative sites is sufficient for agonist-triggered internalization. The observation that internalization and acute shutoff were dissociated by mutation of PAR1 suggests that there are quantitative or qualitative differences in the requirements or mechanisms for these two processes.

Termination of signaling by G protein-coupled receptors (GPCRs)[1] is critical in their biological function (*1*). The thrombin receptor protease-activated receptor 1 (PAR1), a member of the GPCR family, provides an unusual opportunity to study receptor shutoff mechanisms given its proteolytic mechanism of activation (*2*−*4*). Thrombin binds to and cleaves PAR1's amino-terminal exodomain to unmask a new amino-terminal sequence, SFLLRN. This new amino terminus then serves as a tethered peptide agonist, binding intramolecularly to the body of the receptor to effect receptor activation. This irreversible activation mechanism contrasts with that of classical GPCRs, to which ligands can bind and dissociate reversibly. Since PAR1's ligand cannot diffuse away, cleaved receptors might be expected to signal indefinitely. In fact, each receptor signals only briefly (*5*), suggesting the possibility of novel shutoff mechanisms for PAR1. One such mechanism appears to involve PAR1 trafficking. Upon activation by thrombin, most of the cleaved cell surface PAR1 is internalized and sorted to lysosomes for degradation (*6*, *7*). Internalization and degradation of activated PAR1 are critical for preventing activated receptors from remaining on or cycling back to the cell surface (*8*), thereby preventing persistent signaling.

Phosphorylation of PAR1 appears to play an important role in both shutoff and agonist-induced internalization (*9*, *10*). Classical GPCRs become phosphorylated upon activation by G protein-coupled receptor kinases (GRKs) (*1*, *11*,

† This work was supported by National Institutes of Health Grant HL44907. S.R.H. was supported by a postdoctoral fellowship from the Howard Hughes Medical Institute. M.J.S. was supported by a postdoctoral fellowship from the American Cancer Society.

* To whom correspondence should be addressed: HSW-1300, Box 0130, University of California, San Francisco, 505 Parnassus Ave., San Francisco, CA 94143-0130. Telephone: (415) 476-6174. Fax: (415) 476-8173. E-mail: shaun_coughlin@quickmail.ucsf.edu.

‡ Cardiovascular Research Institute.

§ Division of Endocrinology.

|| Department of Medicine.

⊥ Department of Cellular and Molecular Pharmacology.

[1] Abbreviations: GPCR, G protein-coupled receptor; PAR, protease-activated receptor; GRK, G protein-coupled receptor kinase; CM, complete medium; PBS, phosphate-buffered saline; SD, standard deviation.

10.1021/bi9902236 CCC: $18.00 © 1999 American Chemical Society
Published on Web 07/01/1999

12). PAR1 is also rapidly phosphorylated upon activation by thrombin or the agonist peptide SFLLRN (*8*, *10*). When coexpressed with PAR1 in *Xenopus* oocytes, the G protein-coupled receptor kinase GRK3 significantly attenuated thrombin receptor signaling (*10*). Alanine substitution for all threonine and serine residues within PAR1's cytoplasmic tail resulted in a receptor that was insensitive to inhibition by GRK3, as did truncation of the receptor's cytoplasmic tail. These two mutated receptors were not phosphorylated upon activation and signaled more robustly than wild-type receptor (refs *7* and *13* and data not shown). Both mutants were also defective in agonist-triggered internalization (*7*). These data suggest that receptor phosphorylation plays a role in termination of PAR1 signaling but do not address the relative roles of trafficking versus phosphorylation-mediated uncoupling or other mechanisms in PAR1 shutoff.

To identify the phosphorylation sites required for PAR1 shutoff and/or agonist-triggered internalization, we generated mutant receptors in which alanine was substituted for serine and threonine residues in the N-terminal, middle, and C-terminal thirds of PAR1's cytoplasmic tail. Shutoff and internalization of N- and C-terminal substitution mutations were indistinguishable from those of the wild type. Surprisingly, alanine substitution for the middle group of serines yielded a receptor that was relatively defective in shutoff but indistinguishable from the wild type in terms of agonist-triggered receptor internalization and degradation. These results suggest that specific phosphorylation sites are required for rapid receptor shutoff but multiple alternative sites can be sufficient for agonist-triggered internalization. In addition, these results suggest that the rapid shutoff of PAR1 signaling can be dissociated from PAR1 internalization.

MATERIALS AND METHODS

Plasmid Construction. All mutated PAR1s were derived from the human PAR1 bearing a FLAG epitope at its amino terminus (*5*, *14*). Mutations were introduced using the Kunkel method of site-directed mutagenesis (*15*). The oligonucleotide used for S → A (375−392) mutation was 5′-GCTGTTATAAGCGGCGGGATCGGCAGCTTCTTTGCAGCATAAGATAGCATAGACGACCTCTGGCACTCAGCGGCAGCGTAATAG-3′. The oligonucleotide used for S → A (391−406) mutation was 5′-TACTAGAGCATGTATCCATTTAGCTGCCATCAACTGCCCAGCGGCGTTATAAGCGGCGGGATCGGCAGCTTCTTTGCAG-3′. The oligonucleotide used for S/T → A (410−425) mutation was 5′-GTGGTGCTAAGCCAACAGCTTTTTGTATATGGCGTTATTCAGGTTAGCAGCGCAGGCATCCATTTT. Mutations were confirmed by dideoxy sequencing (dRhodamine Terminator Cycle Sequencing Ready Reaction Kit, ABI Prism). cDNAs encoding the wild-type and mutated receptors were subcloned into the mammalian expression vector pBJ (provided by M. Davis, Stanford University, Palo Alto, CA).

Cell Culture and Cell Lines. Rat1 fibroblasts were cultured in complete medium (CM), which consisted of DMEM H-16, 3 g/L glucose, 0.584 g/L L-glutamine, 0.11 g/L sodium pyruvate, and 3.7 g/L $NaHCO_3$, supplemented with 10% BCS, 100 units/mL penicillin, 100 μg/mL streptomycin, and 2.5 μg/mL Fungizone. Rat1 fibroblasts were contransfected with a plasmid encoding the neomycin resistance gene as described previously, and stable cell lines were selected in Geneticin and screened by surface antibody binding of the M1 antibody directed against the FLAG epitope (Kodak) (*7*). All functional studies with mutant receptors were reproduced using cell lines representing two independent clones.

Transient transfections of COS7 cells were performed as described previously (*7*). cDNAs encoding GRK2 and GRK3 were a generous gift from R. Lefkowitz (Duke University, Durham, NC) and were subcloned into the pBJ mammalian expression vector.

Measurement of the Level of Cell Surface Expression. PAR1 on the surface of fibroblasts was detected by cell surface ELISA (*7*). Briefly, cells were incubated at room temperature in DMEM supplemented with 1 mg/mL BSA and 20 mM Hepes (DME/BSA/H) in the presence or absence of 10 nM α-thrombin (Enzyme Research Laboratories) or 100 μM SFLLRN agonist peptide. Cells were fixed at various time points with 4% PFA in PBS for 5 min at 25 °C, followed by two rinses with PBS alone. Cells were then incubated at 25 °C with antibodies directed against the amino terminus of the receptor in DME/BSA/H. Receptors were detected using either the mouse monoclonal M1 anti-FLAG antibody (Kodak) or the 6828 rabbit anti-human PAR1 antibody. This rabbit antiserum was raised to the peptide NATLDPRSFLLRNPNDKYEPFWEDEEGC and recognizes both uncleaved and thrombin-cleaved receptors. After 1 h with the primary antibody, cells were washed twice with PBS and incubated for 30 min at 25 °C with either HRP-conjugated goat anti-mouse or goat anti-rabbit antibodies (Bio-Rad) in DME/BSA/H. Cells were again washed twice with PBS and then incubated in One Step ABTS solution (Pierce) for 10 min. Finally, the absorbance of the supernatant was measured at a wavelength of 405 nm using a Molecular Devices microplate spectrophotometer. Specific modifications in this assay are described in the figure legends.

Phosphoinositide Hydrolysis Assay. The accumulation of [^{3}H]inositol phosphates in response to various agonists was assessed as described previously (*5*, *13*). Briefly, cells expressing the various recombinant PAR1s were incubated overnight with [^{3}H]inositol (Dupont NEN), washed, and treated with or without agonist as described in the figure legends. Lithium chloride (20 mM) was added to block the metabolism of [^{3}H]inositol phosphates. Cells were lysed, and total [^{3}H]inositol phosphates were quantitated (*16*).

Receptor Phosphorylation. Phosphorylation of the recombinant receptors was examined as described previously (*10*). Briefly, cells were plated in six-well dishes (Falcon) and labeled for 3 h at 37 °C with 250 μCi/mL of [^{32}P]-orthophosphate (Dupont NEN) in phosphate-free DMEM. Cells were then washed and incubated with agonist as described in the figure legends. Cells were lysed in 1% Triton X-100, 50 mM Tris-HCl (pH 7.4), 100 mM NaCl, 5 mM EDTA, 50 mM NaF, 20 mM sodium pyrophosphate, 200 μM sodium vanadate, 1 mM PMSF, 1 μg/mL leupeptin, 2 μg/mL aprotinin, 1 μg/mL STI, 1 μg/mL pepstatin A, 1 μg/μL benzamidine, and 10 nM okadaic acid. All chemicals were from Sigma Chemical, except for the okadaic acid (BRL). The M2 antibody (Kodak) was used to immunoprecipitate receptors. Precipitates were resuspended in 2× SDS gel loading buffer [100 mM Tris-HCl (pH 6.8), 4% SDS, 0.2% bromophenol blue, and 20% glycerol], and receptors were resolved on a 10% polyacrylamide gel and analyzed by autoradiography.

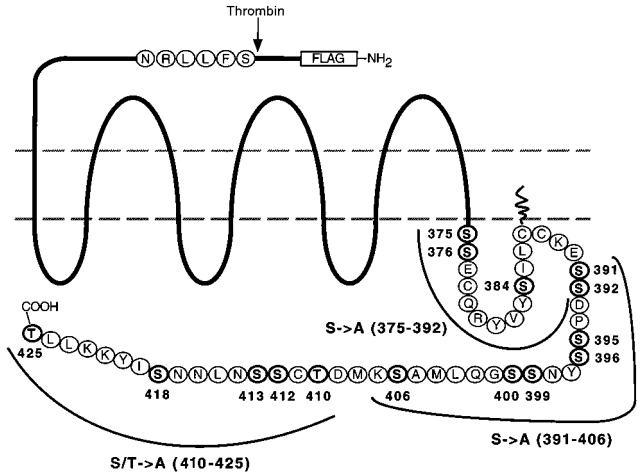

FIGURE 1: PAR1 phosphorylation site mutants. Parallel dashed lines represent the plasma membrane. Extracellular sequences of PAR1 are shown above the plasma membrane. The N-terminal FLAG epitope, thrombin cleavage site, and SFLLRN tethered ligand sequence are denoted. Intracellular domains are shown below the plasma membrane. A putative palmitoylation site at C387 is shown as a wavy line. The amino acid sequence of PAR1's cytoplasmic C-terminal tail is indicated in single-letter code. Serine and threonine residues, potential targets for phosphorylation, are bold and numbered, and alanine substitution mutants are denoted. The mutant receptor designated S → A (375−392) had alanine substituted for serines 375, 376, 384, 391, and 392. S → A (391−406) had alanine substituted for serines 391, 392, 395, 396, 399, 400, and 406. S/T → A (410−425) had alanine substituted for threonines 410 and 425, as well as serines 412, 413, and 418. S/T → A (375−425) (not shown) contained alanines in place of all of the serines and threonines in the cytoplasmic tail.

Immunoblotting. Western blot analysis of both precipitated receptors and whole cell extracts was performed as described previously (*7*, *17*). Samples were resolved by electrophoresis on a 10% polyacrylamide gel. Protein was then transferred to nitrocelluose membranes (Bio-Rad). Membranes were blocked with 5% nonfat dry milk in 50 mM Tris-HCl (pH 7.4), 100 mM NaCl, and 0.1% Tween-20 (TBST) for 1 h, incubated with the rabbit anti-human PAR1 antibody for 2 h (1:2000 dilution of serum), and washed four times with TBST. Blots were then incubated for 1 h with either HRP-conjugated goat anti-mouse antibody (1:10000, Bio-Rad) or 0.5 μCi/mL of [^{125}I]protein A (Amersham). Blots were again washed four times with TBST. Blots exposed to HRP-conjugated antibody were treated with ECL to visualize receptors, while blots incubated with the radiolabeled protein A were analyzed by autoradiography.

RESULTS

Phosphorylation of Recombinant Thrombin Receptors. To determine which phosphorylation targets within PAR1's cytoplasmic tail were important for receptor shutoff and trafficking, groups of serine and threonine residues were changed to alanines (Figure 1). Three mutant receptors containing groups of alanines in place of serine or threonine residues were generated. They were S → A (375−392), which contains alanines in place of serine residues 375, 376, 384, 391, and 392, S → A (391−406), which contains alanines at serine residues 391, 392, 395, 396, 399, 400, and 406, and S/T → A (410−425), which contains alanine substitutions for threonines 410 and 425 and serines 412, 413, and 418. A previously constructed mutant containing alanines in place of all serine and threonine residues within the cytoplasmic tail (*7*, *10*), called S/T → A (375−425), was also used in many of the following experiments.

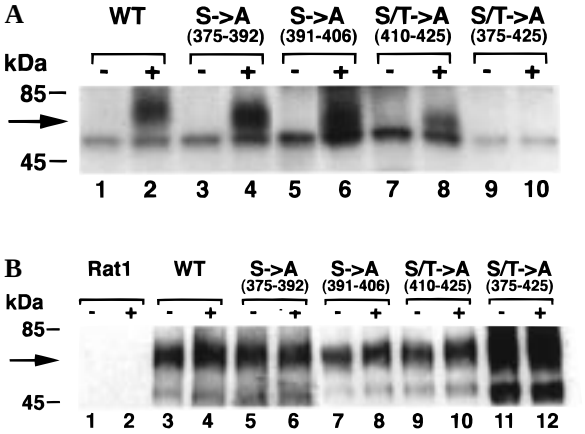

FIGURE 2: Agonist-induced phosphorylation of wild-type and mutated PAR1s. (A) Receptor phosphorylation. Rat1 cells expressing the indicated receptors were labeled with [^{32}P]orthophosphate for 3 h at 37 °C. To have fibroblasts expressing amounts of the S/T → A (375−425) mutant equivalent to wild-type PAR1-expressing cells, a previously made cell line expressing S/T → A (375−425) containing proline in place of the Ser^{42} residue located in the amino-terminal exodomain was used (*7*, *10*). This mutated receptor is no longer activated by thrombin but still responds to SFLLRN agonist peptide; it can be stably expressed at higher levels than S/T → A (375−425) lacking the cleavage site mutation. Cells were then treated for 5 min at 37 °C with either DMEM alone (−) or 100 μM SFLLRN agonist peptide in DMEM (+). The medium was removed; cells were rinsed once with PBS and then lysed. Receptors were immunoprecipitated with M2 antibody directed against an N-terminal FLAG epitope. Immunoprecipitates were analyzed by SDS−PAGE and autoradiography. Phosphorylated PAR1 was detected as a band at approximately 75−80 kDa (arrow). (B) Immunoblot of the samples represented in panel A. Equal volumes of the immunoprecipitates used in the experiments whose results are depicted in panel A were analyzed by immunoblot using rabbit anti-human PAR1 antibody. Note that receptor protein was detected in all immunoprecipitates save the untransfected Rat1 cell negative control. These results were replicated in two separate experiments.

Phosphorylation of the wild-type and mutated thrombin receptors after exposure to agonist was examined. Stable cell lines expressing wild-type PAR1 or one of the four mutated PAR1s were labeled with [^{32}P]orthophosphate followed by incubation with or without the SFLLRN peptide agonist for 5 min. Thrombin receptors were precipitated with the M2 antibody, which recognizes a FLAG epitope engineered into the N-terminus of the recombinant PAR1s (*5*). As expected, wild-type PAR1 was rapidly phosphorylated upon activation by SFLLRN, while phosphorylation of S/T → A (375−425) could not be detected (Figure 2A). S → A (375−392), S → A (391−406), and S → A (410−425) receptors were also phosphorylated in the presence of agonist peptide (Figure 2A). Western blots of these precipitated receptors using a rabbit anti-PAR1 polyclonal antibody confirmed that receptor protein was indeed immunoprecipitated in all cases (Figure 2B). At face value, these results confirm that PAR1's phosphorylation sites are located in the receptor's carboxyl tail and suggest that multiple serines and/or threonines in distinct regions of the tail can be phosphorylated.

Mapping of Phosphorylation Targets That Are Important for PAR1 Shutoff. Signaling and shutoff of PAR1 were examined by measuring the level of phosphoinositide hy-

drolysis in Rat1 cells that had been stably transfected with cDNA encoding wild-type PAR1 or one of the serine/threonine to alanine mutant receptors. Cells that had been labeled overnight with [^{3}H]myoinositol were pretreated for 1 h with 10 nM thrombin in the absence of lithium chloride (LiCl). Under these conditions, phosphoinositides are hydrolyzed, but the resultant inositol phosphates are rapidly degraded. After this incubation, cells were washed and any remaining bound thrombin was blocked with hirudin. LiCl was then added such that ongoing phosphatidylinositol hydrolysis could be detected as accumulation of [^{3}H]inositol phosphates. As expected, little accumulation of inositol phosphates in the presence of LiCl was detected after thrombin removal in fibroblasts expressing wild-type receptors (Figure 3A); thus, signaling by wild-type receptors had largely shut off under these conditions. Signaling in cells expressing mutant receptors with serine/threonine to alanine substitutions in the N-terminal [S → A (375−392)] or C-terminal [S/T → A (410−425)] portions of the tail shut off like signaling in cells expressing wild-type receptors. In contrast, cells expressing the mutant receptor with serine to alanine substitutions in the middle of the C-terminal tail [S → A (391−406)] exhibited persistent signaling after removal of thrombin, releasing [^{3}H]inositol phosphates at a rate that was nearly 70% of that measured when the same cells were simply exposed to thrombin and LiCl simultaneously (Figure 3A). These results indicate that the cluster of seven serines in the middle of the cytoplasmic tail [S → A (391−406)] appears to be necessary for efficient shutoff of signaling, while other potential phosphorylation sites between residues 375 and 392 and between residues 410 and 425 in the carboxyl-terminal tail are not necessary for this function.

We next compared the kinetics of shutoff of S → A (391−406), wild-type PAR1, and S/T → A (375−425), the mutant containing alanine substitutions for all of the serine and threonine residues in PAR1's cytoplasmic tail. Cells expressing each of these receptors were treated with thrombin for various lengths of time in the absence of LiCl. Thrombin was then removed, LiCl added, and any ongoing inositol phosphate accumulation assessed (Figure 3B). As expected, signaling was rapidly attenuated in cells expressing wild-type PAR1. Within 30 min, the level of inositol phosphate accumulation had decreased by 80%. By contrast, cells expressing S/T → A (375−425) continued to signal robustly after removal of thrombin, even after 2 h of previous thrombin treatment. Of note, S/T → A (375−425) was defective in both agonist-triggered phosphorylation (Figure 2A) and agonist-induced internalization and degradation (*7*); thus, this mutant was not informative regarding the relative contributions of acute phosphorylation-dependent uncoupling versus receptor internalization or "downregulation" to termination of signaling. Cells expressing S → A (391−406) exhibited an intermediate phenotype. After 30 min of thrombin exposure, persistent signaling by S → A (391−406)-expressing cells was indistinguishable from that of cells expressing S/T → A (375−425); however, by 120 min, signaling had declined toward wild-type levels. One explanation for this relative defect in overall shutoff in cells expressing S → A (391−406) might be a defect in acute phosphorylation-dependent uncoupling but relatively normal downregulation by internalization and trafficking to lysosomes. To determine whether the phosphorylation site requirements for shutoff might be distinct from those for agonist-triggered internalization, we next examined internalization of wild-type and mutant receptors.

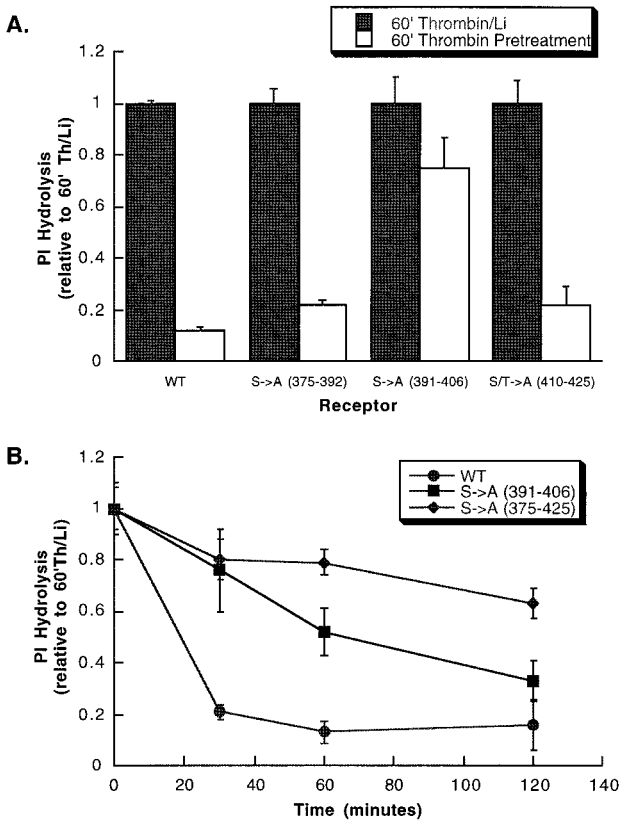

FIGURE 3: Shutoff of signaling by wild-type PAR1 and phosphorylation site mutants. (A) Rat1 fibroblasts expressing either wild-type PAR1, S → A (375−392), S → A (391−406), or S/T → A (410−425) were tested for persistent signaling after incubation with thrombin and its subsequent removal. Cells were labeled overnight with [^{3}H]myoinositol and then pretreated for 1 h at 37 °C in DME/BSA/H containing 10 nM thrombin in the absence of lithium chloride (LiCl). Thrombin was removed; cells were washed three times with DME/BSA/H and then incubated for an additional 60 min at 37 °C in DME/BSA/H containing 20 mM LiCl and 0.5 unit/mL hirudin, a thrombin inhibitor. The levels of accumulated [^{3}H]-inositol phosphates were then measured (white bars). Results were normalized to the value obtained when each cell line was treated with 10 nM thrombin and 20 mM LiCl simultaneously for 60 min at 37 °C (black bars). (B) Kinetics of shutoff of signaling in Rat1 cells expressing wild-type PAR1 (●), S → A (391−406) (■), or S/T → A (375−425) (◆) were examined as described above except that cells were pretreated with 10 nM thrombin for the indicated times, then washed, and incubated for 60 min with LiCl and 0.5 unit/mL hirudin. Note that the S/T → A (375−425) mutant in this experiment contained a wild-type N-terminal exodomain and was capable of being activated in response to both thrombin and SFLLRN agonist peptide. Results for each cell line were again normalized to the quantity of [^{3}H]inositol phosphates measured when cells were incubated for 60 min at 37 °C with both thrombin and LiCl. For cells expressing wild-type PAR1 and S → A (391−406), thrombin and LiCl triggered a 10-fold increase in the level of inositol phosphate accumulation over that with LiCl alone. For cells expressing S/T → A (375−425) a 15-fold increase was observed, and for cells expressing S → A (375−392) and S/T → A (410−425), a 4-fold increase was seen. The level of surface expression of wild-type PAR1 was approximately 15 times the background (nonspecific binding of antibody to untransfected Rat1 cells), approximately twice that of S → A (391−406), approximately 4 times that of S → A (375−392) and S/T → A (410−425), and approximately 6 times that of S → A (375−425). All data depicted in panels A and B are the means ± SD ($n = 3$). The experiments were performed three times with similar results.

Internalization of Wild-Type PAR1 and Phosphorylation Site Mutants. Rat1 fibroblasts stably expressing wild-type PAR1, S → A (375−392), S → A (391−406), or S/T → A (410−425) were treated with thrombin for 1 h, and the amount of receptor remaining on the cell surface was measured using a rabbit polyclonal antibody directed against the hirudin-like domain of PAR1 (Figure 4A). Receptors were completely cleaved within 5 min of thrombin addition as demonstrated by the loss of the FLAG epitope from the cell surface (data not shown). After 1 h in the presence of 10 nM thrombin, the level of surface expression of wild-type PAR1 decreased to approximately half of that seen on untreated cells. Such a decrease in the level of cell surface PAR1 has been shown to correlate with the extent of receptor internalization and does not reflect an altered ability to bind antibody after activation (*18*) (see below). Thrombin treatment of cells expressing any one of the three serine/threonine to alanine mutants resulted in a similar decrease in the level of cell surface expression. Taken together, these data suggest that phosphorylation at several locations within PAR1's cytoplasmic tail is sufficient for mediating agonist-dependent internalization.

Comparison of Wild-Type PAR1 and S → A (391−406) Trafficking. Since the serines between 391 and 406 appeared to be essential for rapid shutoff of PAR1 signaling but not for agonist-induced internalization, we compared the trafficking properties of S → A (391−406) with those of wild-type PAR1 in more detail. Thrombin-induced receptor internalization was examined by treating wild-type PAR1- or S → A (391−406)-expressing cells for various times with 10 nM thrombin and then measuring the extent of binding of receptor antibody to the cell surface. At all the times that were examined, the thrombin-induced decrease in surface levels of S → A (391−406) was at least as robust as that of the wild-type receptor (Figure 4B and data not shown) over time courses relevant to the phosphoinositide hydrolysis studies. Moreover, experiments in which thrombin-triggered decreases in surface receptors were examined revealed similar rates for wild-type PAR1 and S → A (391−406), with approximately half of the total amount of internalization occurring within 5 min for both (data not shown). Similar results were obtained when the exogenous agonist peptide SFLLRN was used to trigger internalization (not shown), suggesting that the decreased level of binding of anti-PAR1 antibody was not simply due to a change in its ability to bind to cleaved receptors. As an alternative to measuring the net decrease in the level of surface expression of receptors (which might reflect both internalization and recycling or synthesis), we also measured the level of SFLLRN-triggered internalization of the surface cohort of receptors (Figure 4C). Again, agonist-triggered internalization of S → A (391−406) and that of wild-type receptors were indistinguishable. Thus, serines between residues 391 and 406 are not necessary for agonist-triggered receptor internalization over the time course that was tested.

We recently demonstrated that lysosomal degradation of activated PAR1 after its internalization is critical for preventing persistent signaling after thrombin activation. Indeed, a PAR1−Substance P receptor chimera that recycled after internalization signaled indefinitely after thrombin cleavage (*8*). Interestingly, mutations of serines in the carboxyl tail of the V2 vasopressin receptor were reported to promote efficient recycling of this receptor to the cell surface (*19*). To test the possibility that the persistent signaling seen with

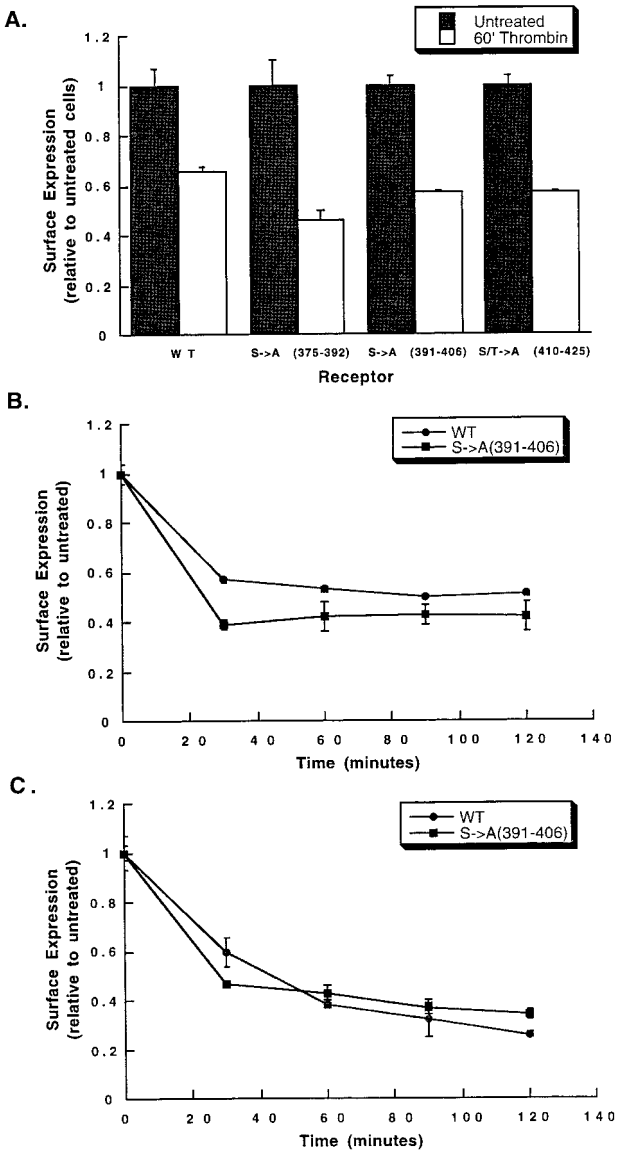

FIGURE 4: Agonist-induced internalization of wild-type and mutated PAR1s. (A) Cells expressing the indicated receptors were treated with either medium alone or medium and 10 nM thrombin for 60 min at 37 °C. Cells were then fixed for 5 min in PBS and 4% paraformaldehyde, washed, and then incubated with rabbit anti-human PAR1 antibody. The amount of bound antibody was measured as an index of receptor remaining on the cell surface as described in Materials and Methods. The amount of receptor detected on the cell surface after thrombin treatment (white bars) was normalized to the amount of surface expression seen in untreated cells (black bars). (B) Kinetics of thrombin-induced reduction of wild-type PAR1 (●) and S → A (391−406) (■) on the cell surface. Cells were exposed to 10 nM thrombin for the indicated periods of time and then fixed; the level of surface expression was measured as described above. (C) Kinetics of agonist-dependent internalization. Cells expressing wild-type PAR1 (●) and S → A (391−406) (■) were labeled with M1 antibody at 4 °C, washed, and then incubated at 37 °C for the indicated periods of time in the presence or absence of 100 mM SFLLRN. Cells were fixed at the indicated times, and the receptor-bound antibody remaining on the cell surface was quantitated as described above. The level of cell surface expression of wild-type PAR1 was twice that of S → A (391−406) and 10-fold above background. The background signal seen with untransfected Rat1 cells was subtracted from each point. Data shown are the means ± SD ($n = 3$). These experiments were performed three times with similar results.

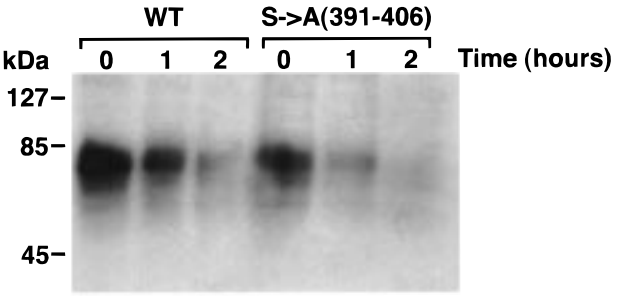

FIGURE 5: Thrombin-induced degradation of wild-type PAR1 and S → A (391−406) receptors. Rat1 fibroblasts expressing either wild-type PAR1 (WT) or S → A (391−406) were treated for 0, 1, or 2 h with 10 nM thrombin in DME/BSA/H and 10 μM cyclohexamide at 37 °C. Cells were lysed in 2× sample buffer as described in Materials and Methods and resolved by SDS−PAGE (10% gel). Proteins were transferred to nitrocellulose, and protein was detected using the rabbit anti-human PAR1 antibody followed by [^{125}I]protein A and autoradiography. PAR1 migrates as a band at approximately 75−80 kDa. The level of expression of wild-type receptors on untreated cells is approximately twice that of S → A (391−406). This experiment was reproduced twice with similar results.

S → A (391−406) might be due to a gain of recycling function and less efficient degradation of activated receptors, we compared degradation and recycling of wild-type and S → A (391−406). Western blot analysis of cycloheximide-treated Rat1 cells expressing wild-type PAR1 revealed a time-dependent decrease in the level of receptor protein after thrombin treatment, reflecting lysosomal degradation of internalized receptors (Figure 5). The decrease in the level of S → A (391−406) after thrombin treatment was similar to that of wild-type PAR1 (Figure 5), suggesting that this mutant is sorted to lysosomes after internalization like the wild type. To determine whether S → A (391−406) gained some increased ability to recycle after activation (thus prolonging signaling), we compared recycling of the internalized wild type and S → A (391−406). M1 antibody was bound to receptor-expressing cells at 4 °C. Cells were then washed, warmed to 37 °C, and incubated for 1 h in the presence or absence of SFLLRN. At this time, antibody remaining on the cell surface was removed by washing with calcium-free PBS containing 0.04% EDTA. Cells were then incubated for 1 h at 37 °C, and the return of antibody−receptor complexes to the cell surface was assessed. Using this assay, we were able to detect robust recycling of Substance P receptors that had undergone agonist-triggered internalization; by contrast, PAR1 exhibited little recycling despite substantial receptor internalization, consistent with internalized PAR1's sorting predominantly to lysosomes (*17*). Both wild-type PAR1 and S → A (391−406) behaved identically in the presence or absence of agonist peptide (Figure 6). In the absence of agonist, the level of surface-bound antibody decreased by 20−30% in 1 h (Figure 6A), consistent with tonic agonist-independent internalization of receptors (*6*, *7*). After removal of cell surface antibody with EDTA and incubation for an additional 1 h, approximately 20% of the original surface cohort of receptor−antibody complexes returned to the cell surface, also consistent with tonic cycling of unactivated receptors (*6*, *7*). Treatment of both cell lines with agonist resulted in the internalization of approximately 80% of cell surface-bound antibody within 1 h (Figure 6B). The extent of recovery of antibody−receptor complexes on the cell surface 1 h after stripping with EDTA

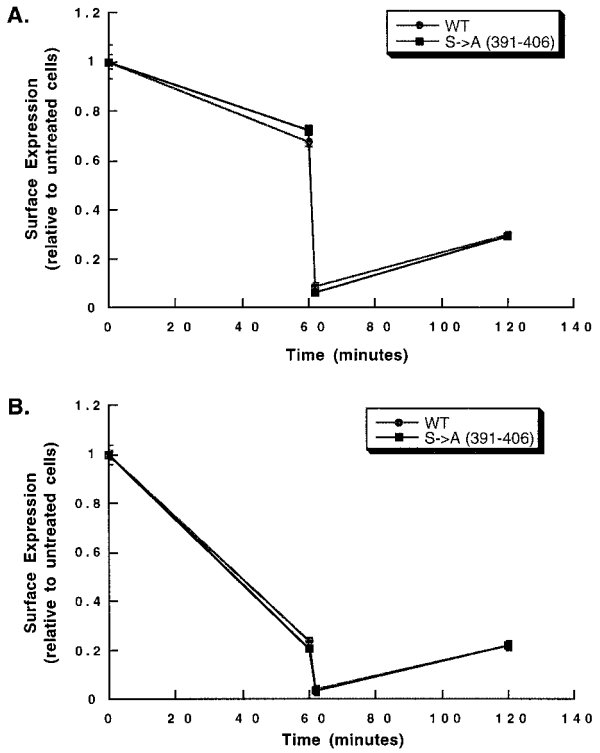

FIGURE 6: Agonist-independent and -dependent trafficking of wild-type PAR1 and S → A (391−406)**.** Cells expressing either wild-type PAR1 (●) or S → A (391−406) (■) were incubated at 4 °C for 60 min in medium containing 1 μg/mL M1 anti-FLAG antibody. Excess antibody was washed away (time zero); cells were warmed to 37 °C, and then samples were incubated in the absence (A) or presence (B) of 100 μM SFLLRN for 60 min at 37 °C (60 min). At this point, cell surface antibody was removed using EDTA (62 min), and cells were incubated for an additional 60 min in medium alone at 37 °C. The reappearance of antibody on the cell surface, a reflection of receptor recycling (*17*), was assessed at this time (120 min). Previous work has demonstrated that the M1 antibody does not significantly dissociate from the receptor under these conditions (*7*) (data not shown). The amount of surface receptor-bound antibody was measured at the indicated times by fixing the cells, incubating with HRP-conjugated goat anti-mouse IgG, and developing with ABTS solution as described in Materials and Methods. The level of surface expression was expressed as a fraction of that in untreated cells. Data shown are the means ± SD ($n = 3$). This experiment was replicated three times with similar results. Note that despite substantial agonist-triggered internalization of both PAR1 and S → A (391−406) (A vs B; 60 min), no increase in the level of recovery of internalized antibody is seen (A vs B; 120 min), suggesting that little recycling of activated receptors occurred.

remained low at approximately 20%, consistent with the majority of activated receptors being sorted to lysosomes (Figure 6B). The lack of a detectable difference between wild-type PAR1 and S → A (391−406) in this assay taken together with their similar rates of degradation (Figure 5) suggests that S → A (391−406) is sorted to lysosomes such as wild-type PAR1 and has not gained any significant ability to recycle to the cell surface after agonist-triggered internalization.

Comparison of the Effects of GRK2 and GRK3 on Wild-Type PAR1 and S → A (391−406) Signaling. When coexpressed with PAR1 in *Xenopus* oocytes, the G protein-coupled receptor kinase GRK3 significantly attenuated PAR1 signaling (*10*). Alanine substitution for all threonine and serine residues within PAR1's cytoplasmic tail resulted in a receptor that was insensitive to inhibition by GRK3. These

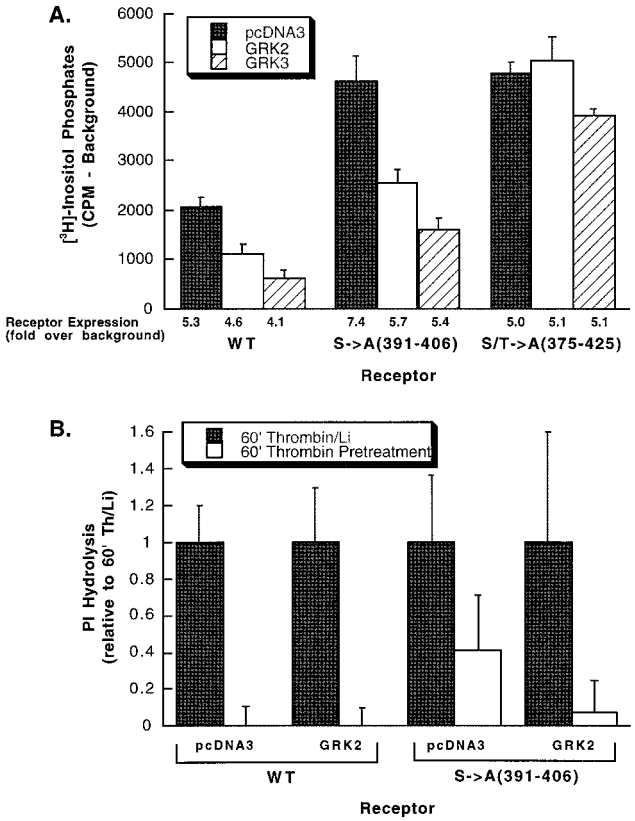

FIGURE 7: Attenuation of signaling of wild-type and mutated PAR1s by GRK2 and GRK3. (A) COS cells were cotransfected with PAR1 expression plasmids and plasmid without insert (black bars) or expression vector for GRK2 (white bars) or GRK3 (hatched bars). After 36 h, cells were labeled overnight with [^{3}H]myoinositol and treated with 10 nM thrombin and LiCl for 45 min at 37 °C. Accumulated [^{3}H]inositol phosphates were then measured and expressed as the increase over inositol phosphate accumulation in cells treated with LiCl alone. Values shown are the means ± SD ($n = 3$). For cells expressing wild-type PAR1, thrombin caused a 3-fold increase in the level of inositol phosphate accumulation, while a 4-fold increase was observed for cells expressing S → A (391−406) and S/T → A (375−425). Surface expression of the wild-type and mutated PAR1s is indicated as the fold increase over background (nonspecific binding of antibody to untransfected COS cells) and is shown below the *x*-axis. Coexpression of GRKs decreased the levels of PAR1 and S → A (391−406) signaling in each of four separate experiments. (B) Shutoff assays were performed as described in the legend of Figure 3 but using COS7 cells cotransfected with either wild-type PAR1 or S → A (391−406) and vector only or a GRK2 expression plasmid. The signal is expressed as the percentage of inositol phosphate accumulation obtained in parallel cultures incubated with thrombin and LiCl for 60 min. In the experiment whose results are shown, the values for fold stimulation were approximately 1.5-fold for cells expressing wild-type PAR1 alone and PAR1 with GRK2, 1.7-fold for S → A (391−406) alone, and 1.4-fold for S → A (391−406) and GRK2. The levels of surface expression of receptors were nearly identical for all transfections in this experiment. Data shown are the means ± SD ($n = 3$). This experiment was performed twice with similar results.

results suggested that GRKs might be important for PAR1 shutoff. We therefore examined the effects of GRK2 and GRK3 on signaling by wild-type PAR1, S → A (391−406), and S/T → A (375−425) in cotransfected COS7 cells (Figure 7). Coexpression of GRK2 or GRK3 significantly attenuated wild-type PAR1 signaling in COS7 cells (Figure 7A). GRK3 was more effective than GRK2 but had a small effect on S/T → A (375−425) signaling, perhaps due to postreceptor actions such as inhibition of $G_{\beta\gamma}$-mediated signaling (*20*, *21*). GRK2 overexpression exhibited no such inhibition of signaling by S/T → A (375−425), consistent with its acting by promoting receptor phosphorylation. Coexpression of either GRK2 or GRK3 with S → A (391−406) resulted in an attenuation of thrombin-mediated signaling that was virtually identical to that seen with wild-type PAR1.

Since GRK2 attenuated signaling by wild-type PAR1 and S → A (391−406), but had no effect of signaling by S/T → A (375−425), we more closely examined the effect of GRK2 on shutoff of PAR1. COS7 cells expressing wild-type PAR1 or S → A (391−406) with or without GRK2 were pretreated with thrombin for 1 h. Thrombin was then removed (and hirudin was added), LiCl added, and inositol phosphate accumulation over the subsequent 60 min assessed as an index of ongoing signaling. Results were compared to the level of inositol phosphates accumulated in 1 h when thrombin and LiCL were simply added simultaneously. As expected, signaling had ceased by this measure in cells expressing wild-type receptor independent of GRK2 overexpression (Figure 7B). By contrast, cells expressing S → A (391−406) exhibited persistent signaling after thrombin removal. Coexpression of GRK2 in cells expressing S → A (391−406) led to nearly complete termination of signaling (Figure 7B). At face value, these results suggest that overexpressed GRK2 can attenuate or terminate thrombin receptor signaling by phosphorylation of serine or threonine residues outside of residues 391−406. This "suppression" of the S → A (391−406) phenotype by GRK overexpression is consistent with the hypothesis that this phenotype results from qualitative or quantitative differences in receptor phosphorylation.

DISCUSSION

Phosphorylation plays a critical role in the rapid uncoupling of activated GPCRs from G proteins (*1*, *9*). Several GPCRs can be phosphorylated at multiple serine or threonine residues in a cytoplasmic loop or the cytoplasmic tail (*22*−*27*). In the case of the β2-adrenergic receptor and rhodopsin (*1*, *12*, *22*−*24*), phosphorylation promotes arrestin binding, which both acutely uncouples the receptor from G protein and, in the case of the β2-adrenergic receptor, promotes internalization. Internalized β2-adrenergic receptor and other reversibly activated GPCRs become dephosphorylated and recycle to the surface, ready to signal again. Thus, internalization of β2-adrenergic receptor is part of a resensitization mechanism.

Like β2-adrenergic receptor and other classical GPCRs, PAR1 is rapidly phosphorylated on serine or threonine residues within its cytoplasmic tail (*7*, *10*). In our current studies, alanine substitution for all serines and threonines in PAR1's cytoplasmic tail ablated agonist-triggered receptor phosphorylation, while alanine substitution of the same residues separately in three distinct clusters yielded receptors that were still phosphorylated (Figure 2). These data show that, like other GPCRs, PAR1 can be phosphorylated at multiple sites after activation. Previous studies showed that phosphorylation sites within PAR1's cytoplasmic tail are necessary for inhibition of PAR1 signaling by the coexpressed G protein-coupled receptor kinase GRK3 (*10*). Furthermore, a receptor missing its targets for phosphory-

lation signaled more robustly than the wild type and was unaffected by coexpression with GRK3 (*7*). In the study presented here, we show that cells expressing one such mutant [S/T → A (375−425)] are defective in shutoff of thrombin signaling. At face value, these data suggest that PAR1 phosphorylation is necessary for termination of PAR1 signaling.

Activated PAR1 is sorted to lysosomes after internalization. This sorting to lysosomes rather than recycling like classical GPCRs is critical for normal termination of PAR1 signaling; thus, in contrast to the case with β2-adrenergic receptor, internalization of activated PAR1 is part of a shutoff mechanism rather than a resensitization mechanism (*6*, *17*). S/T → A (375−425) has a profound defect in its ability to shut off after agonist stimulation. In addition, this mutated receptor is defective in both agonist-triggered phosphorylation and internalization. S/T → A (375−425) is thus uninformative regarding the role of phosphorylation versus receptor internalization in termination of PAR1 signaling. The S → A (391−406) mutant was helpful in this regard. Thrombin signaling in cells expressing this mutant was shut off more slowly than signaling in cells expressing wild-type PAR1, yet wild-type PAR1 and S → A (391−406) were both rapidly phosphorylated after activation and were internalized and degraded at similar rates. These observations suggest that the phosphorylation requirements for rapid shutoff of PAR1 signaling are more stringent than those for agonist-triggered internalization, and that agonist-triggered internalization and degradation of PAR1 are not sufficient for rapid termination of PAR1 signaling. More broadly, they suggest the following model. Activated PAR1 is first uncoupled from signaling by a mechanism requiring phosphorylation of serines between residues 391 and 406. Activated PAR1 is subsequently internalized by a mechanism also requiring phosphorylation of its cytoplasmic tail, but phosphorylation at any of several sites is sufficient. PAR1 internalization and degradation are critical for preventing cleaved and activated PAR1 from remaining on or returning to the surface and "resignaling" but are not sufficient for rapid shutoff of PAR1 signaling**.** The gradual shutoff of signaling after activation of S → A (391−406) (Figure 3) may reflect the contribution of trafficking to the termination of receptor signaling or slower uncoupling via other mechanisms.

Internalization of most GPCRs is coupled to and follows phosphorylation and acute shutoff (*1*, *9*, *11*, *12*), thus, the ability of S → A (391−406) to internalize normally in the presence of a profound defect in acute shutoff is unusual. A similar separation of receptor shutoff from internalization has been seen, however, for the m2 muscarinic acetylcholine receptor, in which serine/threonine → alanine substitutions within the third intracellular loop conferred a desensitization defect in the setting of normal agonist-induced internalization (*25*−*27*). Thus, despite their very different activation mechanisms and fates after internalization, PAR1 and at least one classical GPCR may share a common phosphorylation-dependent uncoupling mechanism with phosphorylation site requirements distinct from those of internalization.

The observation that overexpression of GRK2 suppressed the defect in shutoff of thrombin signaling seen in cells expressing S → A (391−406) suggests that this defect is indeed due to qualitative or quantitative differences in receptor phosphorylation. At least in the case of rhodopsin, receptor phosphorylation alone is not sufficient to prevent G protein activation and signaling (*11*, *22*, *23*, *28*). Rather, receptor phosphorylation promotes its binding to arrestin, and arrestin binding precludes further interaction with G protein. This process is believed to represent the major mechanism by which activated GPCRs are rapidly uncoupled from signaling pathways (*1*, *11*, *12*). Arrestin has also been reported to be a critical mediator of receptor internalization, linking activated receptors to clathrin-coated pits (*1*). This begs the question of how mutation of phosphorylation sites might yield a receptor defective in rapid uncoupling without an accompanying defect in agonist-triggered internalization. One might imagine that internalization may only require that arrestin bind long enough to deliver activated receptors to clathrin-coated pits, while the uncoupling function of arrestin might require a specific and relatively stable structure of the receptor−arrestin complex to prevent receptors from interacting with G proteins. Thus, it is possible that that mutation of some receptor phosphorylation sites might affect the kinetics of arrestin binding or the structure of the receptor−arrestin complex in a way that interferes with uncoupling while leaving internalization intact. Similarly, phosphorylation of some GPCR C-tails at certain sites is thought to promote subsequent phosphorylation at other sites (*29*, *30*); thus, mutating certain sites in PAR1 might alter the kinetics of phosphorylation and arrestin binding such that each activated receptor can signal for a longer period of time. Alternatively, we cannot exclude the possibility that phosphorylation contributes to uncoupling or internalization of PAR1 by mechanisms independent of arrestin binding such that different phosphorylation site mutations would differentially affect these two functions. The role of arrestins in PAR1 shutoff and internalization is not well understood and remains an important question to be studied. The work presented here evokes a testable hypothesis that arrestin binding to S → A (391−406) may be qualitatively or quantitatively different from binding to wild-type PAR1; any such difference would be informative regarding the mechanisms of uncoupling versus internalization.

Last, we cannot exclude the possibility that the shutoff defect of S → A (391−406) is due to a mutation-induced change in the structure of the receptor's cytoplasmic tail rather than to alteration of phosphorylation sites per se. Regardless, the observation that internalization and acute shutoff are dissociated in the S → A (391−406) mutant raises the possibility that there are differences in the mechanisms underlying these two processes and will stimulate inquiry in this area.

REFERENCES

1. Ferguson, S. S. G., Barak, L. S., Zhang, J., and Caron, M. G. (1996) *Can. J. Physiol. Pharmacol. 74*, 1095−1110.
2. Vu, T.-K. H., Hung, D. T., Wheaton, V. I., and Coughlin, S. R. (1991) *Cell 64*, 1057−1068.
3. Coughlin, S. R. (1993) *Thromb. Haemostasis 66*, 184−187.
4. Chen, J., Ishii, M., Wang, L., Ishii, K., and Coughlin, S. R. (1994) *J. Biol. Chem. 269*, 16041−16045.
5. Ishii, K., Hein, L., Kobilka, B., and Coughlin, S. R. (1993) *J. Biol. Chem. 268*, 9780−9786.
6. Hein, L., Ishii, K., Coughlin, S. R., and Kobilka, B. K. (1994) *J. Biol. Chem 269*, 27719−27726.
7. Shapiro, M. J., Trejo, J., Zeng, D., and Coughlin, S. R. (1996) *J. Biol. Chem. 271*, 32874−32880.

8. Trejo, J., Hammes, S. R., and Coughlin, S. R. (1998) *Proc. Natl. Acad. Sci. U.S.A. 95*, 13698−13702.
9. Hausdorff, W. P., Caron, M. G., and Lefkowitz, R. J. (1990) *FASEB J. 4*, 2881−2889.
10. Ishii, K., Chen, J., Ishii, M., Koch, W. J., Freedman, N. J., Lefkowitz, R. J., and Coughlin, S. R. (1994) *J. Biol. Chem. 269*, 1125−1130.
11. Freedman, N. J., and Lefkowitz, R. J. (1996) *Recent Prog. Horm. Res. 51*, 319−353.
12. Premont, R. T., Inglese, J., and Lefkowitz, R. J. (1995) *FASEB J. 9*, 175−182.
13. Nanevicz, T., Wang, L., Chen, M., Ishii, M., and Coughlin, S. R. (1996) *J. Biol. Chem. 271*, 702−706.
14. Gerszten, R. E., Chen, J., Ishii, M., Ishii, K., Wang, L., Nanevicz, T., Turck, C. W., Vu, T.-H. K., and Coughlin, S. R. (1994) *Nature 368*, 648−651.
15. Kunkel, M., and Peralta, E. (1993) *EMBO 12*, 3809−3815.
16. De Vivo, M. (1994) *Methods Enzymol. 238*, 131−140.
17. Trejo, J., and Coughlin, S. R. (1998) *J. Biol. Chem 274*, 2216−2224.
18. Hammes, S. R., and Coughlin, S. R. (1999) *Biochemistry 38*, 2486−2493.
19. Innamorati, G., Sadeghi, H. M., Tran, N. T., and Birnbaumer, M. (1998) *Proc. Natl. Acad. Sci. U.S.A. 95*, 2222−2226.
20. Clapham, D. E., and Neer, E. J. (1997) *Annu. Rev. Pharmacol. Toxicol. 37*, 167−203.
21. Koch, W. J., Hawes, B. E., Inglese, J., Luttrell, L. M., and Lefkowitz, R. J. (1994) *J. Biol. Chem 269*, 6193−6197.
22. Ohguro, H., Van Hooser, J. P., Milam, A. H., and Paleczewski, K. (1995) *J. Biol. Chem. 270*, 14259−14262.
23. Zhang, L., Sports, C. D., Osawa, S., and Weiss, E. R. (1997) *J. Biol. Chem. 272*, 14762−14768.
24. Fredericks, Z. L., Pitcher, J. A., and Lefkowitz, R. J. (1996) *J. Biol. Chem. 271*, 13796−13803.
25. Pals-Rylaarsdam, R., Gurevich, V. V., Lee, K. B., Ptasienski, J. A., Benovic, J. L., and Hosey, M. M. (1997) *J. Biol. Chem. 272*, 23682−23689.
26. Pals-Rylaarsdam, R., and Hosey, M. M. (1997) *J. Biol. Chem. 272*, 14152−14158.
27. Pals-Rylaarsdam, R., Xu, Y., Witt-Enderby, P., Benovic, J. L., and Hosey, M. M. (1995) *J. Biol. Chem. 270*, 29004−29011.
28. Gurevich, V. V., Dion, S. B., Onorato, J. J., Ptasienski, J., Kim, C. M., Sterne-Marr, R., Hosey, M. M., and Benovic, J. L. (1995) *J. Biol. Chem. 270*, 720−731.
29. Onorato, J. J., Palczewski, K., Regan, J. W., Caron, M. G., Lefkowitz, R. J., and Benovic, J. L. (1991) *Biochemistry 30*, 5118−5125.
30. Palczewski, K., and Benovic, J. L. (1991) *Trends Biochem. Sci. 16*, 387−391.

BI9902236